VISUAL MAGNITUDE SATELLITE CATALOGUE RELEASE 1.0

M.D. Hejduk
Titan SenCom Corp., 4575 Galley Road, Colorado Springs, CO 80915
P.W. Kervin, J.V Lambert
Maui Space Surveillance System, 535 Lipoa Parkway, #200, Kihei, Maui, HI 96753
E.G. Stansbury, J.L. Africano
NASA/JSC Houston, TX
E.C. Pearce
MIT Lincoln Laboratory, 244 Wood Street, Lexington, MA 02420

ABSTRACT

The Visual Magnitude Satellite Catalogue Project, sponsored by AFSPC/DOYS, issued the first release of its composite visual magnitude satellite catalogue in July of this year. Some 420,000 raw satellite brightness observations, from both ground- and space-based platforms, were processed to develop statistical brightness characterization and two-parameter brightness models for most of the individual satellites in the deep-space catalogue. This paper discusses the approach and methodology of the effort's model development and provides an assessment of the success and utility of these two-parameter models, concluding that they are adequate for space catalogue brightness characterization and optical sensor scheduling.

1. INTRODUCTION AND DATA DESCRIPTION

The Visual Magnitude Satellite Catalogue project is a collaborative effort among AFSPC, AFRL, NASA, and MIT/LL to combine raw satellite brightness observational data in order to produce a composite, routinely-updated satellite brightness catalogue. Because the contributing agencies are independent and conduct continuous research, it was agreed that each contributor would furnish raw brightness data to AFSPC and receive in return routine updates to the brightness catalogue, but that there would be no cross-distribution of raw data among contributing agencies. The present paper provides a description of the data and processing techniques used to establish the initial delivery of this VM catalogue and attempts some preliminary conclusions regarding the functional relationship between observed brightness and the phase- and solar-declination-angle of the viewing geometry.

For the assembly of release 1.0 of the catalogue, three data sources were available: space-based observations from the SBV (MSX) satellite and ground-based observations from both the SATA demonstration at Edwards AFB, CA and the NASA observing facility at Cloudcroft, NM. SBV collected observations on both near-Earth (NE, orbital period less than 225 minutes) and deep-space (DS, orbital period greater than or equal to 225 minutes) objects but concentrated on DS objects. SATA and Cloudcroft confined themselves to DS objects, with a concentration on geosynchronous objects (orbit class 63, apogee and perigee heights both between 30,000 and 45,000 km).

All three collection efforts often collected multiple brightness observations during a single "look" at a satellite. To treat all the observations within a long track as individuals, equal in weight to perhaps a single observation from a "look" produced from an entirely different viewing geometry, would, for both averaging and curve-fitting, unduly weight those situations in which convenience allowed the collection of long data tracks. Thus, brightness observations that were part of the same track were averaged (in magnitude space) to develop a composite observation that represents the entire track. For SATA and Cloudcroft, whose raw data come accompanied with some calibration information, track boundaries were easy to identify by looking for changes in this accompanying calibration information. The form in which the SBV data were supplied did not contain analogous calibration information, so this track boundary identification approach could not be used. An examination of the data revealed that observations that appeared to be part of the same viewing session generally were separated in time by less than five minutes. Thus, the decision was made to amalgamate SBV observations on the same object that differed in time by less than fifteen minutes (actually, 0.01 of a day, 14.4 minutes). Because SATA and Cloudcroft use identical calibration and observation-processing software, are both ground-based sensors, and together contribute a minority of the observations, it was often found convenient to group them together into a single dataset, given the title "SACL." The data on DS objects available from all three sources for catalogue assembly, in both pre- and post-

amalgamated form, are summarized in Table 1, and the portions of the deep-space and geosynchronous objects observed are given in Fig 1. A distinction is drawn between the presence of any data at all and a non-sparse sample (here taken to be > 30 observations) from which averaging and curve-fitting can be expected to be more meaningful.

Table 1: Pre- and post-amalgamation observation counts

Sensor	Data Date Range	Pre-Avg Obs Count	Post-Avg Obs Count
SBV	6/6/96 – 9/30/00	271,772	187,528
SATA	8/15/99 – 12/31/99	148,062	32,132
Cloudcroft	3/1/98 – 12/31/99	6,833	5,253

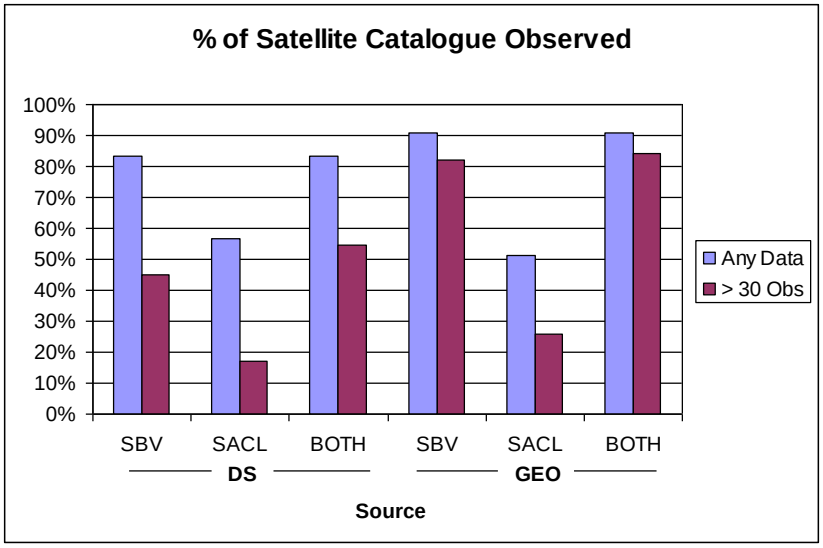

Fig. 1

2. PHOTOMETRIC CALIBRATION AND FRAME-WEIGHTING

Large variations are often observed in the quality of individual data-frames, so it is desirable to conduct averaging and curve-fitting in a weighted manner, with the weighting factors derived from the frame's photometric calibration results. The canonical four-factor photometric calibration equation is given as:

$$V = m_0 - k'm - k''Cm + \varepsilon C + \zeta \,, \qquad (1)$$

in which k' is the atmospheric extinction coefficient, k'' the color-dependent atmospheric extinction coefficient, ε the color transformation term, and ζ the zero-point offset. Ideally, all four calibration constants would be computed for each frame, allowing a fully normalized result to be obtained; unfortunately, calibration to this fidelity is rarely accomplished in actual operations. The SATA system, which of the three systems supplied the most complete calibration results, calculated only the zero-point offset, absorbing all the atmospheric and color dependencies into a single term. However, despite this abbreviated *modus operandi*, SATA does provide with each observation the zero-point offset applied and the zero-point standard deviation resulting from its calculation. This latter quantity is well-suited to serve as a weighting factor. A typical zero-point standard deviation for SATA data hovered around 0.3 magnitude, which is a reasonable estimate of the average error of such data. Because the Cloudcroft observations are processed with the same software, these same weights are in principle available; but unfortunately they were not explicitly produced as part of the forwarded data reduction. If they can be produced from archived calibration information, then the catalogue averages and curve-fits can be re-generated for improved accuracy. SBV produces as part of its calibration procedures a calibration RMS. Perhaps this RMS can be used in a similar manner to the zero-point offset standard deviation as a weighting factor; whether these RMSs can be recovered for existing observations is still under investigation. For the present catalogue, default weights of 0.3 magnitude were assigned to all Cloudcroft and SBV data.

Concerns about the color compatibility among the three observing platforms are very real. If all three platforms were to choose solar-equivalent stars for their photometric calibrations, then the results would be less idiosynchratic but not free of all color compatability issues, as the satellites themselves are not solar-colored. Unfortunately, even this more modest level of compatability may be difficult to attain, as many frames do not contain enough solar-equivalent stars to allow a durable calibration, forcing augmentation with stars with non-negligible B-V and V-R terms. The MIT/LL CCD has a known, characterized color bias, and transformation equations have been developed to correct for this. At the present time, it is not known whether sufficient descriptive data about the individual SBV calibration frames have been preserved to allow these transformations to be applied *ex post facto*. Because of these potential incompatibilities, averages and curve-fits for each object have been calculated in three ways: using only SBV data, using only SACL data, and using both data sets mixed together (assigned the term "BOTH"). If users determine that color incompatabilities between the two types of observing platforms make the combination of their data unwise, they can elect to use fit-results calculated from only SBV or SACL data.

Previous studies have investigated and attempted to model the onset and severity of satellite specular response as solar phase angles approach zero [1,2]. The developed models from these studies show, in magnitude space, departure from linear response (with solar phase angle as independent variable) between phase angles of ten and fifteen degrees. Based on this modeling, an argument could be made to eliminate low-phase-angle data from any averaging and curve-fitting that is trying to model diffuse response. Further work is needed to determine how much of an effect such an exclusion would have on the present effort; for the initial production of the catalogue, it was thought appropriate to maximize the data pool by making all data available for averaging and curve-fitting. It should be pointed out that only 3.4% of the observations were taken at phase angles smaller than 10 degrees and only 11.2% for phase angles smaller than 15 degrees, so an extreme biasing of the outcome due to the presence of these low-phase-angle data is unlikely.

3. STATISTICAL CHARACTERIZATION

Averaging was straightforward. For each data set a weighted mean, weighted (sampling) standard deviation, and unweighted median were calculated, all in magnitude space. For objects that cannot produce any statistically-significant curve fits, the weighted mean is suggested as the best predictor of future brightness, invariant with phase and solar declination angle. It has been presumed that the data sets for such objects follow a normal distribution (for sample sizes > 30 obs), but the propriety of this presumption is still to be verified explicitly. Although simple weighted means and standard deviations were used in all cases, future catalogue editions will probably employ instead a student's *t*-distribution for lightly-sampled satellites. A weighted mean phase and solar declination angle are also calculated; these were seen as a way to describe an "average" viewing geometry for the object. While the limitations to this approach are clear enough, it does appear to be the recommended procedure for describing the average viewing geometry for asteroids, at least in terms of phase angle [3].

4. MODEL DEVELOPMENT

As has been presumed but perhaps not sufficiently laid out in the preceding discussion, satellite illumination is being analyzed in a satellite-centered reference frame, with its resultant brightness considered as a function of three possible illumination angles. Solar phase angle is the angle formed by the sun, the satellite, and the observing platform, with the satellite at the vertex. A phase angle of 0 degrees describes a situation in which the light source and the observing platform are directly aligned, producing the greatest observed brightness; as the angle moves to 180 degrees, the illumination becomes more oblique until 180 is reached, at which point the part of the satellite facing the sensor is not illuminated at all. For a diffuse sphere, positive and negative phase angles are equivalent; for an asymmetric or materially heterogeneous satellite, they can be notably different. However, since none of the three observing platforms used for this version of the catalogue reports a signed phase angle, these distinctions could not be considered in catalogue assembly. Solar declination angle considers the effect of the tilt of the earth's axis on satellite illumination: geosynchronous satellites will be "bottom-lit" for negative solar declination angles and "top-lit" for positive ones. For a diffuse sphere, solar declination has no effect on resultant brightness; but the effects can be significant for an asymmetric satellite. A third angle, called the obliquity angle, relates to the angle between the unit normal of the satellite's principal surface and that of the observing sensor's focal plane. Because spacecraft orientation and rotation rates must be known in order to determine this latter angle

for each observation, it was not used in the present analysis. For three-axis-stabilized geosynchronous active payloads, solar phase and declination angles provide a reasonably complete description of the variables affecting resultant brightness; for other DS satellites, or for observations taken from space-based platforms, the geometrical issues become more complex. The research question to be answered here is whether the two parameters of solar phase angle and solar declination angle can reasonably be used, for the purposes of satellite catalogue characterization and sensor scheduling, to predict brightnesses for these more complex geometries.

Curve-fitting was thus pursued for all objects in the following way. First, multiple regression was attempted (in magnitude space), with solar phase angle (α) and solar declination angle (δ) as linear regressor variables. The linear variation of brightness with solar phase angle is predicted by the diffuse spherical model and has been verified empirically for selected types of objects [4]. A similar canonical behavior is expected for solar declination angle variations. Of course, satellite material properties, spacecraft configuration, and payload mounting asymmetries will all cause variation from the theoretical prediction; but the theoretical response seemed a good overall model form to use. The results of this multiple regression for each object were examined to determine if they passed a 0.05 significance *F*-test. If so, a 0.05 significance *t*-test was performed against each of the three regressor coefficients, with special attention paid to the two variable regressor constants. If it was determined that both variables contributed significantly to the regression, the two-variable fit was the fit-form used for this object. If only one of the two variables was determined to contribute significantly, then the regression was re-run with only that one variable as a regressor variable. If neither variable contributes significantly (indicated initially by an *F*-test failure), then no further curve-fitting is attempted; for such objects, averages are recommended as the most useful statistical descriptors.

5. MODEL EVALUATION

It is not a difficult task to write software to attempt/accomplish curve-fitting; whether the resultant models are ultimately useful as a description of the overall data set is what needs to be determined. To answer this broader question, several sub-questions are prompted. First, how should the data from these two disparate data sets—space-based and ground-based—be treated? Despite the different observing paradigm, calibration approach, and color systems, is it still preferable to combine the data from both sources and process them together, thus being able to proceed from a larger data pool; or should they remain segregated, producing separate space- and ground-based catalogues? Second, what is the preferred functional form for curve-fitting? A linear relationship between brightness (in magnitude space) and phase angle has been established for certain classes of satellites, but how widely applicable is this relationship among different orbits and spacecraft? Separately, rather little has been done to explore the form and tenacity of the relationship between brightness and solar declination angle; can certain basic aspects of this relationship be established, at the least as a foundation for further enquiry? Finally, the ability of a curve-fit to pass significance thresholds is no guarantee of its being widely representative; do the statistically-significant fit results possess enough representational ability to give them real predictive value to determine optimal scheduling of sensor resources?

The first step to answering these questions is to examine comparatively how well each data type responded to curve-fitting in terms of producing statistically-significant curve-fits. Fig. 2 shows how the three data types—SBV alone, SACL alone, and SBV and SACL combined (BOTH)—fared for both DS generally and GEO orbits specifically, with both more and fewer than thirty observations. The y-axis is the percent of satellites with data in the relevant orbital regime (DS or GEO) for which a curve-fit against α, δ, or $\alpha + \delta$ was statistically significant. It quickly becomes apparent that requiring a thirty-observation minimum renders a significant improvement in curve-fitting success, although this improvement is less marked in GEO, where the data density is higher and fewer undersampled cases exist. In the GEO region, the combined data case is able successfully to fit slightly more satellites than that for SBV alone, but it is interesting that in the well-sampled DS case this is not true—SBV alone actually does slightly better than the BOTH case. Still, the differences are not significant enough either to recommend or prohibit the combination of data from the two. As would be expected, fitting is improved, in many cases significantly, by requiring a thirty-sample minimum; the subsequent discussion of curve-fitting successes and failures is limited to these more plentifully-endowed cases.

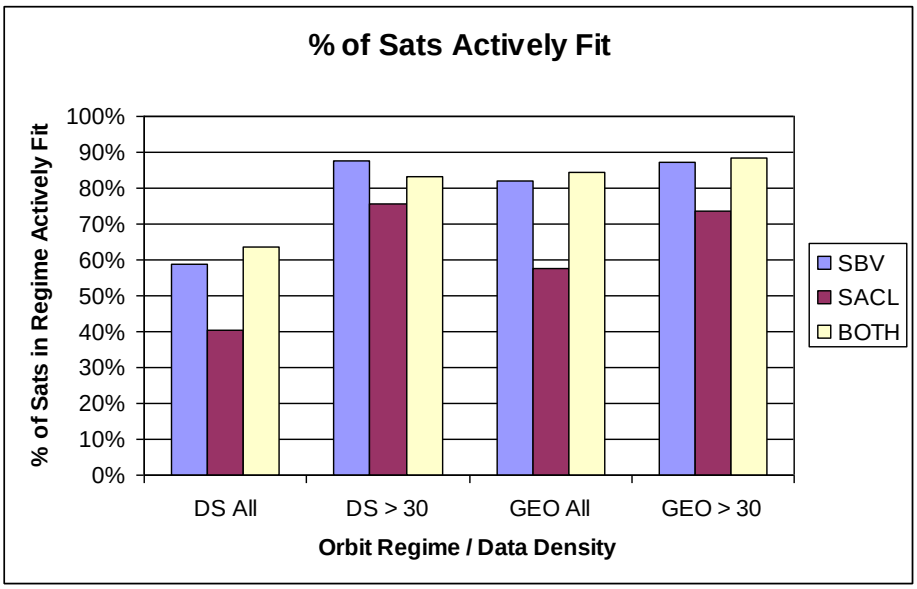

Fig. 2

Fig. 3 shows the successes of different fitting combinations, called here "fit-states," as a function of data group. Fit-state "No" indicates that no fit was possible, α indicates that a fit against only solar angle was successful, δ indicates that a fit against only solar declination angle was successful, and $\alpha + \delta$ indicates that a fit including both α and δ as regressor variables was successful. Any given satellite can be placed in only one of these bins, with the exception of "Tot", which represents all successful fits taken together.

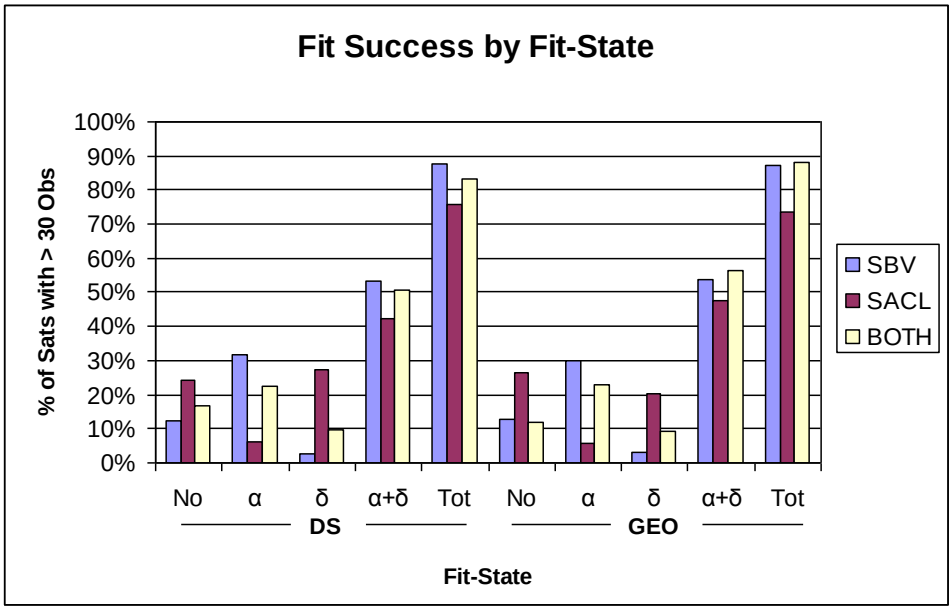

Fig. 3

These results yield several interesting features and confirm certain suppositions. First, because SBV takes observations on geosynchronous satellites from many more viewing geometries than are possible for a ground-based sensor, one would expect observed brighnesses to correlate more strongly with solar phase angle than with solar declination angle; and in fact the results bear this out: 30% of the cases produce a statistically-significant fit with α alone, as opposed to *ca*. 3% with δ alone. It did somewhat exceed expectations, however, to see so large a number

of cases (53%) fit to both α and δ, showing that while α may be the predominant predictor, δ should not be neglected, as it still contributes significantly to the majority of fits. Second, for the ground-based fits derived from SACL observations, δ becomes the predictor of choice, outperforming α for single-parameter fits by at least a factor of three. This comes as something of a surprise, as one might have expected a more even apportionment of influence between α and δ; but in the end, as with SBV, using both α and δ as regressor variables was the most successful strategy overall. However, one must be cautious in forming conclusions about the relative influence of α and δ on SACL observations because of systematic relationships between the two parameters: in order to maximize the probability of acquisition, the observing α and δ are not chosen randomly and independently but in a coupled manner expected to produce the brightest return. Not necessarily the best, but certainly the simplest, defense against the colinearity this phenomenon can introduce is to combine these SACL data with the SBV data, which do not suffer from this systematic effect, to form a larger, heteronomous data pool. Indeed, it can be seen that the combined data pool ("BOTH" in Fig. 3) fares better *vis-à-vis* fit success, in both DS generally and GEO specifically, than the SACL data; in comparison to the SBV data, a slight penalty is exacted in DS generally but a slight improvement in GEO specifically. Thus, in terms of fit success, there is no obvious penalty to using the combined data set, and a particular advantage if SACL colinearity can be addressed. What remains to be seen is whether there is any meaningful discrepancy in the quality of the fits themselves.

Fig. 4 shows the r^2 and standard error results for fits against α, δ, and $\alpha + \delta$. Because of space limitations, only the results for GEO are shown here; but the results for the broader DS case are similar in form. The purpose of these charts is to show quality of fit comparatively for each fit-type (for example, how do the fits against α only compare in quality among the SBV, SACL, and combined data sets, in terms of both r^2 and SEE?); to show comparative quality among the α, δ, and $\alpha + \delta$ cases; and to show absolutely the quality of fits obtained by this technique. The data are graphed as cumulative percentile charts in order to normalize for the different numbers of objects fit by each fit-type.

The left-hand graphs in Fig. 4 show the relative goodness-of-fit among the three data pools in each fit-state and among the three fit-states, and a correlation is seen immediately between the number of satellites successfully fit to a given fit-state from a given data pool and the quality of that fit. For example, in the top-left graph, which plots r^2 for α alone as the regressor variable, it is clear that the fits obtained from SACL data are not nearly so good as those obtained from the SBV and BOTH data pools; and in fact far fewer statistically-significant fits against α alone were produced (as was shown in Fig. 3). When δ is the lone regressor variable, the situation is reversed, as shown in the left-middle graph; better fit quality is observed for the SACL data pool than for the SBV and BOTH pools, and indeed far more satellites from the SACL pool were successfully fit to δ alone than from the SBV or BOTH pools. More homogeneity is present in the $\alpha + \delta$ case; the results for the BOTH pool reside between those for the SBV and SACL.

Table 2 attempts to summarize these r^2 results; it should be read as shown in the following example: "70% of the fits of the SBV GEO data set against α alone achieved an r^2 better than or equal to 0.26."

Table 2: GEO regression results by percentile and regressor variable

Regressor Variables	Data Source	50th Percentile		70th Percentile		90th Percentile	
		r^2	r	r^2	r	r^2	r
α	SBV	0.39	0.62	0.26	0.51	0.11	0.34
	SACL	0.09	0.30	0.07	0.26	0.02	0.16
	BOTH	0.36	0.60	0.22	0.47	0.08	0.29
δ	SBV	0.10	0.32	0.08	0.28	0.03	0.18
	SACL	0.29	0.53	0.17	0.41	0.05	0.22
	BOTH	0.10	0.32	0.08	0.28	0.03	0.17
$\alpha + \delta$	SBV	0.38	0.62	0.24	0.49	0.09	0.30
	SACL	0.24	0.49	0.16	0.40	0.08	0.29
	BOTH	0.28	0.53	0.20	0.44	0.08	0.28

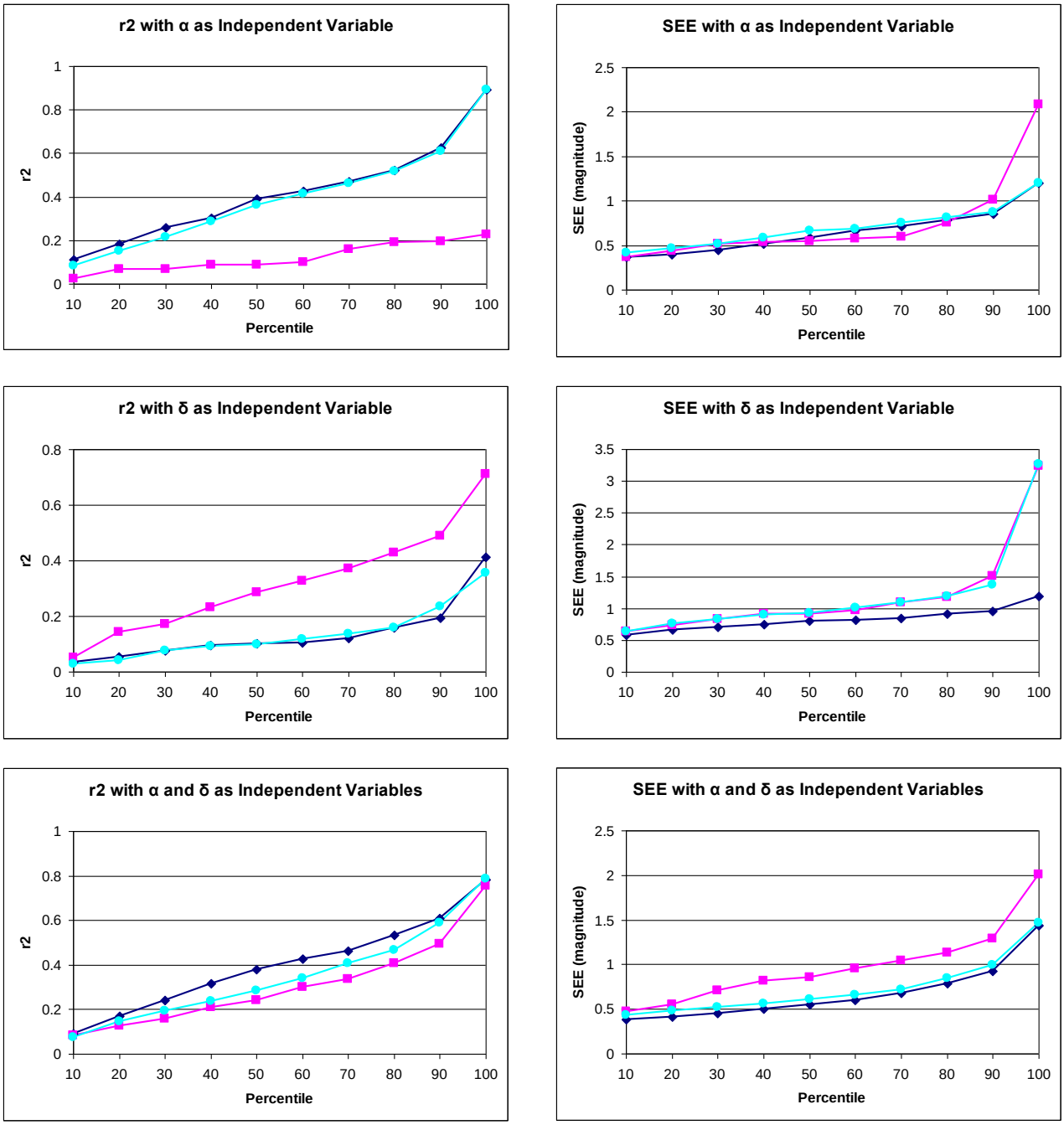

Fig. 4 (diamonds denote SBV, squares SACL and circles BOTH)

Looking at the results comparatively, the combination of data sets (the BOTH category) produces an r^2 between that for SBV and SACL, with SBV leading in some cases and SACL in others. In some cases the r^2 difference between the combined data pool and the better of the two individual data pools is notable (*e.g.*, δ as regressor, 50th percentile, SACL's 0.29 compared to BOTH's 0.10). However, the differences are not substantial; and when one considers the broader application of the BOTH data set and the mitigation of colinearity, it still can be advanced as the set of results appropriate to most catalogue users.

Regarding the association between absolute r^2 values and the conclusion that the fit is adequate or inadequate, there seems to be no consensus in engineering applications. Within the social sciences, however, there is more of an established framework for such an association, although it is based on the Pearson correlation coefficient (r) rather than its square (r^2). The following mapping of heuristic quality-of-fit descriptions to Pearson values has been proposed [5]:

Table 3: Mapping among r^2 value, Pearson value, and heuristic fit assessment

Heuristic Description	Pearson Value	r^2 Equivalent
Slight, almost negligible relationship	< .20	< .04
Low correlation; definite but small relationship	.20 - .40	.04 - .16
Moderate correlation; substantial relationship	.40 - .70	.16 - .49
High correlation; marked relationship	.70 - .90	.49 - .81
Very high correlation; very dependable relationship	> .90	> .81

For the combined data pool, the results for all three regressor combinations at the 50th percentile fall within (or are at the boundary of) the "substantial relationship" case; and at the 70th percentile, all but the lightly-populated "δ-alone" case still achieve this. These statistically-significant fits seem to be of enough stature to recommend their use as preferable to the simple averaging of all the data for a satellite.

There is in general less variation among the different data pools regarding standard errors (SEE) than was observed with r^2. For the α-alone and δ-alone cases, SEE's generated from the three data pools remain quite close together until the 90th percentile is reached; for the $\alpha + \delta$ case, SACL lags the other two cases by about half a magnitude. Table 4 summarizes these SEE results for percentile ranks of interest:

Table 4: SEE results by percentile, data pool, and regressor variables

Regressor Variables	Data Source	50th Percentile	70th Percentile	90th Percentile
None	SBV	0.81	0.92	1.06
	SACL	0.99	1.14	1.66
	BOTH	0.94	1.08	1.38
α	SBV	0.59	0.71	0.85
	SACL	0.55	0.60	1.01
	BOTH	0.66	0.75	0.87
δ	SBV	0.80	0.85	0.96
	SACL	0.92	1.10	1.50
	BOTH	0.92	1.09	1.37
$\alpha + \delta$	SBV	0.55	0.68	0.93
	SACL	0.86	1.04	1.29
	BOTH	0.61	0.72	1.00

Again, the δ-alone case produces the least satisfactory results; but the better-populated cases of α-alone and $\alpha + \delta$ produce, at the 50th percentile, standard errors slightly over half a magnitude, working their way up to a full magnitude by the 90th percentile. Such results are hardly so satisfactory that one can declare victory and prescind from any further refinements in the fit-model; indeed, model refinement will be among the visual magnitude satellite catalogue project's chief activities as the project proceeds. However, the fit-results for the present version of the catalogue and its associated models are strong enough to recommend these models for space catalogue brightness characterization and optical sensor scheduling.

6. REFERENCES

1. Lambert, J.V., "Interpretation of Geosynchronous Satellite Phase Angle versus Magnitude Relationships", Contract F05603-90-C-0010 Specialized Data Report: MOTIF FY95-01, 30 NOV 1994.

2. Lambert, J.V., "Analysis of Magnitude versus Phase Angle Data for Two Classes of Deep Space Satellites", Contract F05604-95-C-9011 Specialized Data Report: MSSS FY96-04, 11 OCT 1996.

3. Bowell, E., Hapke, B., Domingue, D., Peltoniemi, J., and Harris, A., "Application of Photometric Models to Asteroids", *Asteroids II*, University of Arizona Space Science Series, Binzel, Gehrels, and Matthews, general editors, Tucson, AZ: University of Arizona Press, 1990, pp. 524-556.

4. Lambour, R.L., "Phase Angle Dependence of Satellite Brightness Derived from Space-Based Visible Data," MIT/LL Project Report SPC-8, 20 FEB 2001.

5. Guilford, J.P., *Fundamental Statistics in Psychology and Education*, New York: McGraw Hill, 1956.